JOURNAL OF ALLOYS AND COMPOUNDS
SUBMITTED MANUSCRIPT

Letter

Incorporation of platinum atoms in a silicon-free boride of the YB_{50}-type structure

Oksana Sologub[1,*], Leonid P. Salamakha[1], Berthold Stöger[2], Peter F. Rogl[3], Herwig Michor[1], Ernst Bauer[1]

[1]Institute of Solid State Physics, TU Wien, A-1040 Wien, Austria
[2]Institute for Chemical Technologies and Analytics, TU Wien, A-1040 Wien, Austria
[3]Institute of Materials Chemistry and Research, University of Vienna, A-1090 Vienna, Austria

Abstract

A new Pt-doped yttrium boride of the YB_{50} family, $YB_{45-x}Pt_y$, x=2.12, y=0.21 (space group *Pbam*, a=16.6246(4) Å, b=17.6453(4) Å, c=9.4167(2) Å), has been synthesized by arc-melting pure elements and subsequent annealing at 1123 K. A single crystal has been studied in order to assess the Pt-doping effect on the crystal structure. Insertion of Pt in two 4*h* interstitial sites of the boron atom framework leads to the transformation of -[B_{12}]-[B_{12}]- icosahedral chain into -[B_{11}]-Pt-[B_{11}]- for 38.6% of them as well as, to a lesser extent, induces the disorder into the [B_{15}] polyhedron and neighboring interstitial B site (97.3% *vs* 2.7%).

Keywords: boride; transition metal; single crystal X-ray diffraction; $YB_{45-x}Pt_y$.

* Corresponding author *E-mail address: oksana.sologub@univie.ac.at.*

1. Introduction

Boron-rich solids constitute an important class of materials with useful physical properties such as chemical inertness, high temperature stability and high hardness. Among them, [B_{12}] icosahedral compounds attract considerable interest as promising candidates for high temperature thermoelectric conversion due to their high melting temperatures and low values of thermal conductivity [1-3]. It was until 1990th when Tanaka *et al*. [4-6] discovered two new phases in the boron rich part of the Y-B system, i.e. YB_{25} and YB_{50}, that REB_{12} and REB_{66} (RE - rare earth element) were thought to be the only boron-rich rare-earth borides. Novel compounds were found to form isotypic structures with heavy rare earth (RE) elements (RE=Y, Gd-Lu) as well as exhibited the ability to incorporate light element atoms (C, Si). Incorporated atoms of light elements tend both to reside in the voids of the icosahedral boron framework interconnecting the boron clusters (alike in the $YB_{25}C$ and its superstructures [7]), as well as to occupy certain sites within the boron polyhedral units, as for example, in compounds with a general formula $REB_{44}Si_x$ which originate from the REB_{50} structure [6,8]. YB_{50} decomposes at 1973 K, thus making it difficult to grow sizable single crystals for physical properties investigations. The addition of Si was reported to enable coexistence of the YB_{50} phase with melt, resulting in successful crystal growth by the floating zone method [8]. It was also concluded from electron probe microanalysis data that, similarly to *rh* β-B and YB_{66}, the YB_{50} structure uptakes a considerable amount of transition element atoms (Co, Ni, etc.; e.g. Y/Ni ratio was observed to reach 0.8/0.2) [8]. This valuable property of the framework of boron atoms could be exploited to enhance the crystallinity of the RE higher borides of the YB_{50} family as well as to modify their thermoelectric properties. Recently, the properties of differently doped $YB_{44}Si_2$:T samples (T = Ti, V, Mn, Fe, Cu, Zn, Mo, Rh) have been reported; among them the Zn doping was found to improve the thermoelectric power factor of the yttrium borosilicide by more than 30% [9,10]. The mechanism of insertion of transition metal elements into the boron atom framework was studied from X-ray single crystals for only Ni- and Rh-doped yttrium boron silicides [11] while no information exists on the structural features and physical properties of silicon-free platinum doped yttrium borides of the YB_{50} family. According to binary phase diagram studies [12,13], the platinum borides have low melting tempeartures and may serve as a flux agent for high temperature solution growth of the platinum containing RE higher borides. Our work on synthesis and structural studies of boron rich phases in the Y-Pt-B system revealed a new platinum doped yttrium boride featuring a complex boron atom framework of YB_{50}. Current experiments yielded crystal grains sufficient for structural studies, the results of which are presented below.

2. Experimantal details

In order to evaluate the formation of boron-rich phases in the Y-Pt-B system (>75 at. % B), several samples were synthesized by argon arc-melting appropriate amounts of pieces of yttrium (Alfa Aesar, purity 99.9 mass%), platinum foil (Ögussa, 99.9%,) and crystalline boron (ChemPur, Germany, 99.8 mass%). The arc melted buttons were wrapped in tantalum foil and vacuum-sealed in quartz tube for heat treatment at 1123 K for 1 week. The X-ray powder diffraction (XPD) patterns of the samples located in the adjacent to Y-B boundary concentration range revealed mainly a mixture of highly stable binaries (YB_{66} and YB_{12}), however the XPD patterns of both as cast and annealed samples with higher platinum content (>10 at. % Pt) exhibited, except the peaks belonging to the Pt_3B_2 phase, a pronounced array of reflections similar to the pattern reported for YB_{50} [8]. X-ray single crystal intensity data were collected for the best quality specimen selected from the $Y_3Pt_{18}B_{79}$ alloy using a Bruker APEX II diffractometer (CCD detector, κ-geometry, Mo Kα radiation); orientation matrix and unit cell parameters were derived with the help of the program DENZO [14]. Multi-scan absorption correction was applied using the program SADABS; frame data were reduced to intensity values employing the SAINT-Plus package [15]. The structure was solved by direct methods (SHELXS-97 [16]) and refined by full-matrix least-square structure refinement (SHELXL-97 [17]). The refined atom coordinates were standardized with the program STRUCTURE TIDY [18]. Further details concerning the crystal structure investigation are listed in Table 1.

3. Results and discussion

The space group *Pbam* was indicated by the systematically absent reflections [19]. Direct methods delivered a structure solution with two sites for metal atoms, namely Y and Pt, however a high value of isotropic displacement parameter for the Pt atom site hinted towards a fractional population which was further refined to about 39%. The remaining atom sites (Table 1) were found from difference Fourier maps after subsequent refinement of heavy atom positions according to reasonable interatomic distances between detected and proposed atoms (Table 2). The refinement converged to a reliability factor value of 0.0336 exhibiting the residual electron densities within -0.80 e/Å^3 and 1.97 e/Å^3.

$YB_{45-x}Pt_y$, x=2.12, y=0.21 is the first Pt-doped member of the orthorhombic YB_{50} structural family. According to Tanaka *et al.* [6,8], the atom framework of related silicon boride $YB_{41}Si_{1.2}$ consists of five [B_{12}] icosahedra and a 15-member unit with the actual formula [$B_{12}Si_{1.5}B_{1.5}$] where three split atom sites are statistically occupied by either boron or

silicon. Y atoms are located in the large voids of the boron atom framework. The unit cell of $YB_{41}Si_{1.2}$ also includes seven B interstitial sites (two 8-fold and five 4-fold) exhibiting occupancies varying from 100% to 8% and one interstitial Si site (4*h*) occupied up to 80% thus delivering a general formula $YB_{45-x-y}Si_ySi_{0.4}$. A recent study of Berthebaud *et al.* [11] on Rh- or Ni-doped yttrium boron silicides confirmed in general the distribution of boron and silicon within the boron atom framework, however revealed additionally the partially occupied transition metal atom site. The insertion of Rh (or Ni) in interstitial 4*h* site led to the transformation of $[B_{12}]$ icosahedra into $[B_{11}]$ polyhedra in a disordered fashion (i.e. B in 8*i* occ. 0.96 *vs.* Rh in 4*h* occ 0.04).

In contrast to $YB_{41}Si_{1.2}$ and Rh- or Ni-doped yttrium boron silicide structures [6,11], no Si atoms have been encountered both in icosahedral / polyhedral and interstitial sites of Pt-doped yttrium boride as deduced from refinement of occupancy parameters and analysis of electron density maps. The fact of silicon absence on boron atom sites in the current structure is well supported by the reduced value of the unit cell volume of Pt-doped yttrium boride (2762.3 $Å^3$) as compared to the volumes of pure $YB_{41}Si_{1.25}$ and Rh- or Ni-doped yttrium boron silicides (2800.7 $Å^3$, 2800.3 $Å^3$ and 2809.5 $Å^3$, respectively). Yttrium atoms reside in voids created by boron icosahedra; besides there are eight 4-fold boron populated interstitial sites which yield occupancies varying from 100% to 25% (Table 1). A structural analysis revealed the layered arrangement of polyhedra along the *z*-axis. The layer in the *z*=0 plane is composed of three types of icosahedra (A, B and C in Fig. 1a); at *z*=½ one can find the icosahedron D and $[B_{15}]$ polyhedron E (Fig. 1b). The polyhedron F is located at *z*=¼; F polyhedra condense along *c*-axis to form infinite chains (Fig. 1c) which bridge the nets of polyhedra located at *z*=0 and *z*=½. In agreement with Rh- and Ni-doped yttrium boron silicide [11], the refinement on $YB_{45-x}Pt_y$, x=2.12, y=0.21 single crystal data revealed the split of the apical site of the $[B_{12}]$ icosahedron F (B01 in 8*i* (*x*, *y*, *z*; *x*=0.3127(3), *y*=0.3401(3), *z*=0.4157(6)) and Pt01 in 4*h* (*x*, *y*, ½; *x*=0.31097(2), *y*=0.34202(2), z=½)) (Fig.1d) demonstrating, however, higher Pt occupancy as compared to Rh- and Ni-doped yttrium boron silicide (Pt01 in 4*h*, occ.= 0.386(1) vs. Rh or Ni in 4*h,* occ.=0.04 and occ.=0.12, respectively) (Fig. 2). Additionally, in the course of refinement, the difference Fourier map displayed a prominent electron density (~8.3 e/$Å^3$) in 4*h* (*x*~0.15, *y*~0.015, *z*=½) corresponding to an interstitial Pt02 site at about 0.93 Å from B02 of the $[B_{15}]$ polyhedron and at 1.12 Å from bridging B39 atom (Fig. 2 b-c). Reasonable distances and displacement parameters for this site could only be achieved through partial occupancy of B and Pt sites. A refinement of occupancies of B02/B39/Pt02 converged at filling levels of 97.4% B02 and 97.4% B39 vs 2.6% Pt02 indicating occasional presence of

either the [B_{15}] polyhedron (E) (Fig. 1b) and eight interstitial B sites or of the [B_{13}] unit, Pt02 and seven interstitial boron sites (Fig. 1d).

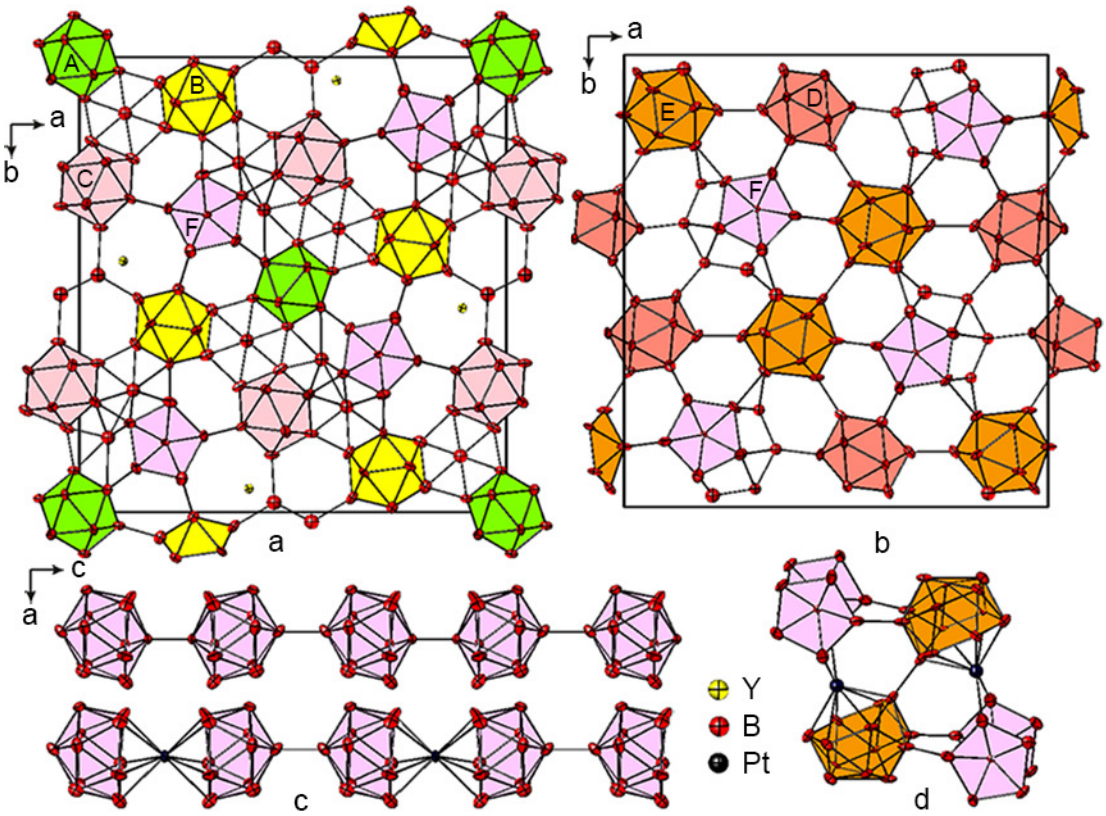

Fig. 1. Crystal structure of $YB_{45-x}Pt_y$, x=2.12, y=0.21 as seen along the *c*-axis within -0.25≤*z*≤0.25 (a) and 0.25≤*z*≤0.75 (b). Linkage of [B_{12}] and [B_{11}] units along *c*-axis in case of boron (8*i*) and platinum (4*h*) partial occupancy (c). Bonding scheme in case of insertion of Pt in 4*h* (*x*,*y*,½; *x*=0.1545(4), *y*=0.0155(3)) atom site (d).

4. Conclusions

In summary, YB_{50}-type compounds have been hitherto reported to incorporate certain amounts of transition elements, i.e. Co, Ni and Rh. We report here for the first time on platinum doping of a silicon-free higher boride of the YB_{50} family. X-ray single crystal diffraction showed that the new compound crystallizes in space group *Pbam* (No. 55) with lattice constants a=16.6246(4) Å, b=17.6453(4) Å, c=9.4167(2) Å). Partial split of in total three boron sites into two platinum sites leads to the formula $YB_{45-x}Pt_y$, x=2.12, y=0.21. The behavior of Pt as a dopant differs considerably from that of Rh and Ni in terms of the atom sites adopted and with respect to the filling levels of atom positions occupied by the transition metal. Since the main negative influence on the thermoelectric properties of $REB_{44}Si_x$ is the

relatively high resistivity, the observed substantial Pt doping may have a beneficial effect on the power factor via lowering the resistivity. A possibility of transition metal heavy doping of YB_{50} structure stimulates the further work on a single crystal growth of the new higher boride with the aim of exploration of physical properties.

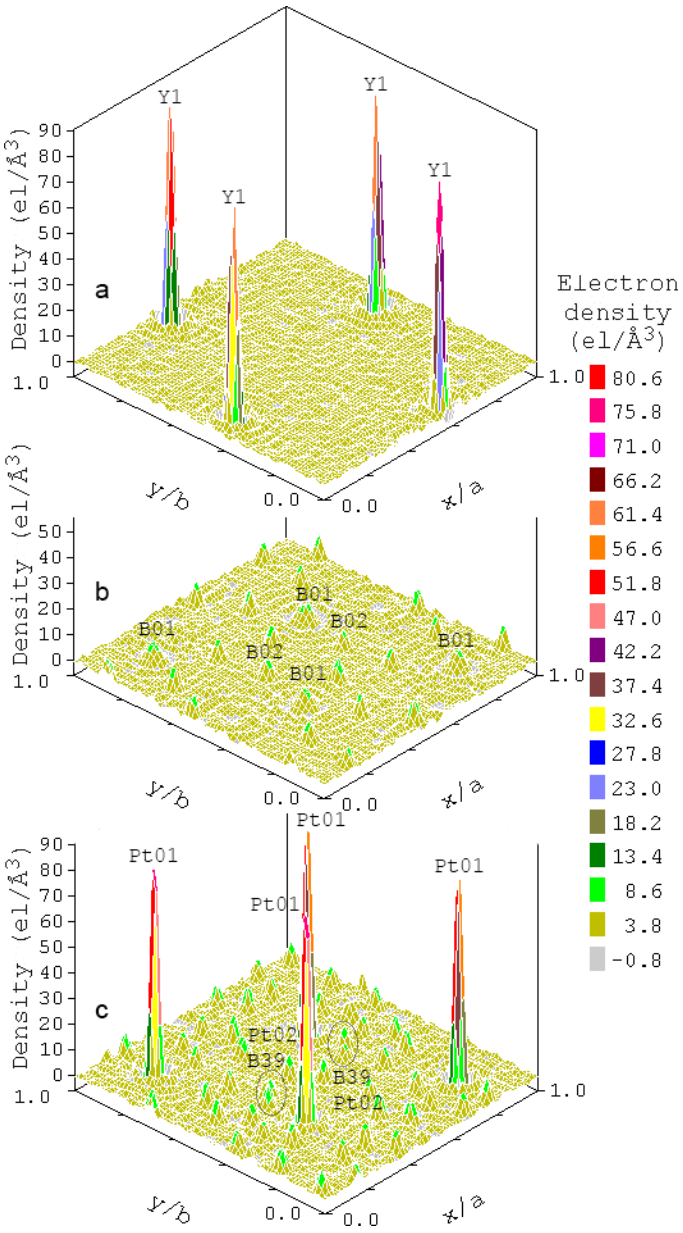

Fig. 2. F_{obs} Fourier maps at z≈0.41 (b) and z≈0.5 (c) emphasizing the electron densities corresponding to atoms in split positions. Yttrium atoms plane (z≈0.24) (a) is given for comparison.

Acknowledgements

The research work of O.S. was supported by Austrian FWF project V279-N19. Authors are very thankful to Dr. Klaudia Hradil (XRC TU Wien) for collaboration.

References

[1] H. Werheit, Boron and Boron-rich Compounds, in: Y. Kumashiro (Ed), Electric Refractory Materials, Marcel Dekker Inc. , New York, 2000, pp. 589-653.

[2] H. Werheit, Solid State Sciences 13 (2011) 1786-1796

[3] T. Mori, Higher Borides, in: K. A. GschneidnerJr., J.-C. Bunzli, V. Pecharsky (Eds.), Handbook on the Physics and Chemistry of Rare Earths, vol. 38, North- Holland, Amsterdam, 2008, pp. 105–173.

[4] T. Tanaka, S. Okada, Y. Yu , Y. Ishizawa, J. Solid State Chem. 133 (1997) 122-124.

[5] T. Tanaka, S. Okada, Y. Ishizawa, J. Alloys Compd. 205 (1994) 281-284.

[6] I. Higashi, T. Tanaka, K. Kobayashi, Y. Ishizawa, M. Takami, J. Solid State Chem. 133 (1997) 11-15.

[7] F.X. Zhang, F.F. Xu, A. Leithe-Jasper, T. Mori, T. Tanaka, A. Sato, P. Salamakha, Y. Bando, J. Alloys Comp. 337 (2002) 120–127.

[8] T. Tanaka, S. Okada, Y. Ishizawa, J. Solid State Chem. 133 (1997) 55-58.

[9] T. Mori, T. Shishido, K. Nakajima, J. Electr. Mat. 38(7) (2009) 1098-1103.

[10] T. Mori, D. Berthebaud, T. Nishimura, A. Nomura, T. Shishido, K. Nakajima, Dalton Trans. 4 (39) (2010) 1027–1030.

[11] D. Berthebaud, A. Sato, Y. Michiue, T. Mori, A. Nomura, T. Shishido, K. Nakajima, J. Solid State Chem.184 (2011) 1682–1687.

[12] T.B. Massalski, in Binary Alloy Phase Diagrams, ASM International, Materials Park, OH, 2nd edn., 1990.

[13] O. Sologub, L.P. Salamakha, P.F. Rogl, B. Stöger, E. Bauer, J. Bernardi, G. Giester, M. Waas, R. Svagera, Inorg. Chem, 2015, 54 (22), 10958–10965.

[14] Bruker Advanced X-ray solutions. APEX2 User Manual. Version 1.22. 2004, Bruker AXS Inc.

[15] Bruker. APEXII, SAINT and SADABS. 2008, Bruker Analytical X-ray Instruments, Inc., Madison, Wisconsin, USA.

[16] G.M. Sheldrick, SHELXS-97, Program for the Solution of Crystal Structures; University of Göttingen, Germany, 1997.

[17] G.M. Sheldrick, SHELXL-97, Program for Crystal Structure Refinement; University of Göttingen, 1997.
[18] E. Parthé, L. Gelato, B. Chabot, M. Penzo, K. Censual and R. Gladyshevskii, TYPIX – Standardized Data and Crystal Chemical Characterization of Inorganic Structure Types; Berlin: Springer, 1994.
[19] Farrugia, L.J. J. Appl. Cryst. 32 (1999) 837.

Table 1

X-ray single crystal data for $YB_{45-x}Pt_y$, x=2.12, y=0.21[a].

Formula from refinement	$YB_{42.88}Pt_{0.21}$
Nominal composition	$Y_{2.3}B_{97.2}Pt_{0.5}$
Space group, Z	*Pbam* (No.55), 8
Structure type	Pt-doped YB_{50}
Diffractometer	Bruker APEX II
Range for data collection (deg)	$2.16<\theta<30.06$
Crystal size	40x45x35 μm^3
a (Å), *b* (Å), *c* (Å)	16.6246(4), 17.6453(4), 9.4167(2)
a (Å), *b* (Å), *c* (Å) (XPD data)	16.6197(9), 17.6418(10), 9.4187(5)
Reflections in refinement	3416 $F_o > 4\sigma(F_o)$ of 4272
Mosaicity	<0.4
Number of variables	384
$R_F^2 = \Sigma\|F_0^2-F_c^2\|/\Sigma F_0^2$; R_{Int}; GOF	0.0336; 0.042; 1.066
Extinction (Zachariasen)	0.0001(1)
Residual density; max; min (el/Å^3)	1.97; -0.80
Y1 in 8*i* (*x*,*y*,*z*); occ.; U_{eq}[b,c]	*x*=0.10261(2), *y*=0.44854(1), *z*=0.23491(3); 1.00; 0.282(8)
B1 in 8*i* (*x*,*y*,*z*); occ.; U_{eq}	*x*=0.0164(2), *y*=0.3226(2), *z*=0.1642(3); 1.00; 0.43(6)
B2 in 8*i* (*x*,*y*,*z*); occ.; U_{eq}	*x*=0.0335(2), *y*=0.0385(2), *z*=0.1583(3); 1.00; 0.42(6)
B3 in 8*i* (*x*,*y*,*z*); occ.; U_{eq}	*x*=0.0631(2), *y*=0.2304(2), *z*=0.1606(3); 1.00; 0.45(6)
B4 in 8*i* (*x*,*y*,*z*); occ.; U_{eq}	*x*=0.0685(2), *y*=0.0779(2), *z*=0.3074(3); 1.00; 0.42(6)
B5 in 8*i* (*x*,*y*,*z*); occ.; U_{eq}	*x*=0.0816(2), *y*=0.1773(2), *z*=0.3082(3); 1.00; 0.40(6)
B6 in 8*i* (*x*,*y*,*z*); occ.; U_{eq}	*x*=0.1193(2), *y*=0.3114(2), *z*=0.0987(3); 1.00; 0.40(6)
B8 in 8*i* (*x*,*y*,*z*); occ.; U_{eq}	*x*=0.1681(2), *y*=0.1149(2), *z*=0.3086(3); 1.00; 0.43(4)
B9 in 8*i* (*x*,*y*,*z*); occ.; U_{eq}	*x*=0.1686(2), *y*=0.2010(2), *z*=0.4081(3); 1.00; 0.43(4)
B10 in 8*i* (*x*,*y*,*z*); occ.; U_{eq}	*x*=0.2079(2), *y*=0.3328(2), *z*=0.1854(3); 1.00; 0.37(6)
B11 in 8*i* (*x*,*y*,*z*); occ.; U_{eq}	*x*=0.2247(2), *y*=0.3837(2), *z*=0.3486(3); 1.00; 0.48(6)
B12 in 8*i* (*x*,*y*,*z*); occ.; U_{eq}	*x*=0.2257(2), *y*=0.1003(2), *z*=0.1602(3); 1.00; 0.33(6)
B13 in 8*i* (*x*,*y*,*z*); occ.; U_{eq}	*x*=0.2395(2), *y*=0.2797(2), *z*=0.3359(3); 1.00; 0.51(6)
B14 in 8*i* (*x*,*y*,*z*); occ.; U_{eq}	*x*=0.2602(2), *y*=0.4260(2), *z*=0.1855(3); 1.00; 0.51(4)
B15 in 8*i* (*x*,*y*,*z*); occ.; U_{eq}	*x*=0.2675(2), *y*=0.0101(2), *z*=0.0987(3); 1.00; 0.40(6)
B16 in 8*i* (*x*,*y*,*z*); occ.; U_{eq}	*x*=0.2879(2), *y*=0.2585(2), *z*=0.1773(3); 1.00; 0.47(6)
B17 in 8*i* (*x*,*y*,*z*); occ.; U_{eq}	*x*=0.2878(2), *y*=0.1738(2), *z*=0.0965(3); 1.00; 0.37(6)
B18 in 8*i* (*x*,*y*,*z*); occ.; U_{eq}	*x*=0.2964(2), *y*=0.3469(2), *z*=0.0878(3); 1.00; 0.37(6)
B19 in 8*i* (*x*,*y*,*z*); occ.; U_{eq}	*x*=0.3252(2), *y*=0.4312(2), *z*=0.3373(3); 1.00; 0.51(4)
B20 in 8*i* (*x*,*y*,*z*); occ.; U_{eq}	*x*=0.3330(2), *y*=0.0864(2), *z*=0.1638(3); 1.00; 0.35(6)
B21 in 8*i* (*x*,*y*,*z*); occ.; U_{eq}	*x*=0.3501(2), *y*=0.2628(2), *z*=0.3308(3); 1.00; 0.53(6)
B22 in 8*i* (*x*,*y*,*z*); occ.; U_{eq}	*x*=0.3671(2), *y*=0.4037(2), *z*=0.1790(3); 1.00; 0.51(6)
B23 in 8*i* (*x*,*y*,*z*); occ.; U_{eq}	*x*=0.3815(2), *y*=0.3046(2), *z*=0.1729(3); 1.00; 0.46(6)
B24 in 8*i* (*x*,*y*,*z*); occ.; U_{eq}	*x*=0.3836(2), *y*=0.0933(2), *z*=0.3356(3); 1.00; 0.35(5)
B25 in 8*i* (*x*,*y*,*z*); occ.; U_{eq}	*x*=0.3920(2), *y*=0.1877(2), *z*=0.4058(3); 1.00; 0.42(5)
B26 in 8*i* (*x*,*y*,*z*); occ.; U_{eq}	*x*=0.4032(2), *y*=0.3557(2), *z*=0.3324(3); 1.00; 0.48(6)
B27 in 8*i* (*x*,*y*,*z*); occ.; U_{eq}	*x*=0.4350(2), *y*=0.4511(2), *z*=0.0957(3); 1.00; 0.42(5)
B28 in 8*i* (*x*,*y*,*z*); occ.; U_{eq}	*x*=0.4628(2), *y*=0.2585(2), *z*=0.0964(3); 1.00; 0.36(6)
B29 in 8*i* (*x*,*y*,*z*); occ.; U_{eq}	*x*=0.4739(2), *y*=0.0455(2), *z*=0.4065(3); 1.00; 0.36(5)
B30 in 8*i* (*x*,*y*,*z*); occ.; U_{eq}	*x*=0.4815(2), *y*=0.1426(2), *z*=0.3359(3); 1.00; 0.40(5)

B31 in 8*i* (*x*,*y*,*z*); occ.; U_{eq}	*x*=0.4989(2), *y*=0.3671(2), *z*=0.4070(3); 1.00; 0.46(5)
B32 in 4*h* (*x*,*y*,½); occ.; U_{eq}	*x*=0.0329(3), *y*=0.0408(3); 1.00; 0.49(8)
B33 in 4*h* (*x*,*y*,½); occ.; U_{eq}	*x*=0.0375(3), *y*=0.3843(3); 1.00; 0.40(5)
B34 in 4*h* (*x*,*y*,½); occ.; U_{eq}	*x*=0.0454(3), *y*=0.2138(3); 1.00; 0.46(5)
B35 in 4*h* (*x*,*y*,½); occ.; U_{iso} [c]	*x*=0.1417(3), *y*=0.3724(3); 0.91(2); 0.44(8)
B36 in 4*h* (*x*,*y*,½); occ.; U_{iso}	*x*=0.1821(3), *y*=0.2854(3); 0.84(2); 0.44(8)
B37 in 4*h* (*x*,*y*,½); occ.; U_{iso}	*x*=0.1905(3), *y*=0.4599(3); 0.93(2); 0.44(8)
B38 in 4*h* (*x*,*y*,½); occ.; U_{eq}	*x*=0.2206(3), *y*=0.1218(3); 1.00; 0.43(6)
B40 in 4*h* (*x*,*y*,½); occ.; U_{eq}	*x*=0.3270(3), *y*=0.1217(3); 1.00; 0.43(6)
B41 in 4*h* (*x*,*y*,½); occ.; U_{eq}	*x*=0.3767(3), *y*=0.0343(3); 1.00; 0.46(8)
B42 in 4*h* (*x*,*y*,½); occ.; U_{eq}	*x*=0.4882(3), *y*=0.2022(3); 1.00; 0.48(9)
B43 in 4*g* (*x*,*y*,0); occ.; U_{eq}	*x*=0.0121(3), *y*=0.0917(3); 1.00; 0.37(6)
B44 in 4*g* (*x*,*y*,0); occ.; U_{eq}	*x*=0.0297(3), *y*=0.1855(3); 1.00; 0.40(6)
B45 in 4*g* (*x*,*y*,0); occ.; U_{iso}	*x*=0.0438(3), *y*=0.4789(3); 1.00; 0.41(8)
B46 in 4*g* (*x*,*y*,0); occ.; U_{eq}	*x*=0.0492(3), *y*=0.3745(3); 1.00; 0.40(6)
B47 in 4*g* (*x*,*y*,0); occ.; U_{eq}	*x*=0.0930(3), *y*=0.0297(3); 1.00; 0.37(6)
B48 in 4*g* (*x*,*y*,0); occ.; U_{iso}	*x*=0.1075(8), *y*=0.1233(7); 0.37(2); 0.5(2)
B49 in 4*g* (*x*,*y*,0); occ.; U_{eq}	*x*=0.1249(3), *y*=0.2231(3); 1.00; 0.40(6)
B50 in 4*g* (*x*,*y*,0); occ.; U_{eq}	*x*=0.1894(3), *y*=0.0556(3); 1.00; 0.44(8
B51 in 4*g* (*x*,*y*,0); occ.; U_{eq}	*x*=0.2016(3), *y*=0.1548(3); 1.00; 0.46(7)
B52 in 4*g* (*x*,*y*,0); occ.; U_{eq}	*x*=0.3614(3), *y*=0.0314(3); 1.00; 0.45(6)
B53 in 4*g* (*x*,*y*,0); occ.; U_{eq}	*x*=0.3686(3), *y*=0.1311(3); 1.00; 0.45(6)
B54 in 4*g* (*x*,*y*,0); occ.; U_{eq}	*x*=0.4571(3), *y*=0.1724(3); 1.00; 0.40(6)
B55 in 4*g* (*x*,*y*,0); occ.; U_{iso}	*x*=0.4327(8), *y*=0.3358(8); 0.33(2); 0.5(2)
B56 in 4*g* (*x*,*y*,0); occ.; U_{iso}	*x*=0.3741(10), *y*=0.2319(10); 0.25(2); 0.5(2)
B01 in 8*i* (*x*,*y*,*z*); occ.; U_{eq} or	*x*=0.3127(3), *y*=0.3401(3), *z*=0.4157(6); 0.614(1); 0.26(1)
Pt01 in 4*h* (*x*,*y*,½); occ.; U_{eq}	*x*=0.31097(2), *y*=0.34202(2); 0.386(1); 0.26(1)
B02 in 8*i* (*x*,*y*,*z*); U_{iso} [c]	*x*=0.1412(2), *y*=0.0306(2), *z*=0.4099(4); 0.973(1); 0.76(5)
B39 in 4*h* (*x*,*y*,½); occ.; U_{iso} or	*x*=0.2910(3), *y*=0.4749(3); 0.973(1); 0.76(5)
Pt02 in 4*h* (*x*,*y*,½); occ.; U_{iso}	*x*=0.1545(4), *y*=0.0155(3); 0.027(1); 0.76(5)

[a] formula accounts for unoccupied interstitial boron atom site 4*g* (*x*,*y*,0) x≈0.25, y≈0.24 which is populated for 46% in $YB_{41}Si_{1.2}$ [6]; [b] equivalent isotropic (U_{eq}) and isotropic (U_{iso}) atomic displacement parameters ($Å^2 \times 10^2$); [c] anisotropic displacement parameters are listed in CIF file deposited with Fachinformationszentrum Karlsruhe, 76344 Eggenstein-Leopoldshafen, Germany (e-mail: crysdata@fiz-karlsruhe.de) with depository numbers CSD-430598.

Table 2

Selected bond lengths (Å) in $YB_{45-x}Pt_y$, x=2.12, y=0.21.

Atom - ligand	Bond length (min; max)
Y-B	2.478(2) - 2.948(3)
Pt-B	2.070(8) - 2.559(5)
B-B (intraicosahedron A)	1.609(5)-1.802(6)
B-B (intraicosahedron B)	1.731(5)-1.883(4)
B-B (intraicosahedron C)	1.717(7)-1.877(4)
B-B (intraicosahedron D)	1.729(6)-1.881(4)
B-B (intraicosahedron F)	1.654(6)-1.963(5)
B-B (intrapolyhedron E)	1.731(6)-2.017(4)
B-B[a]	1.599(9)-1.827(5)
B-B[b]	1.633(9)-2.07(2)
B-B[c]	1.66(1)-2.042(5)

[a] intericosahedral/interpolyhedral bonds; [b] bonds between atoms in interstitial sites; [c] bonds between atoms in interstitial and polyhedral sites